J Fluoresc (2015) 25:777–785
DOI 10.1007/s10895-015-1587-0

FLUORESCENCE NEWS ARTICLE

Solvent and pH Effects of Coumarin-Terminated Monolayer on Silver Particles

Issha Nadirah Ismail[1] · **Nurul Izzatil Aisya Asri**[1] · **Hairul Anuar Tajuddin**[1] · **Zanariah Abdullah**[1]

Received: 9 February 2015 / Accepted: 26 May 2015 / Published online: 9 June 2015

Abstract A coumarin-terminated self-assembled monolayer on silver particles (**C-SAM**) from the reduction of silver ions in the presence of compound **3** was successfully prepared by utilizing phase transfer method, and analyzed by FTIR, SEM-EDS, UV-Visible and a particle sizer. The fluorescence behavior of coumarin termini was carried out in ethanol and chloroform with emission wavelength determined at 386 nm, suggesting an interaction between the carbonyl group and the solvent media. The dispersion was then investigated in acidic and basic conditions, showing a direct proportional correlation between the emission and the pH of the aqueous. These results were consistent for interpreting hydrogen bonds, particularly between the carbonyl group with either proton of the alcohol (C=O——H-O-R) or positive species in acidic conditions (C=O——H^+). The interactions were possible only when the coumarin terminal rearranged in the monolayer and the carbonyl exerted towards the solvent media, while the rest of the molecules were separated from the solvents.

Keywords Self-assembled monolayer · Fluorescence · Coumarin · Polar environment

Electronic supplementary material The online version of this article (doi:10.1007/s10895-015-1587-0) contains supplementary material, which is available to authorized users.

✉ Issha Nadirah Ismail
issha89@siswa.um.edu.my

[1] Department of Chemistry, Faculty of Science, University of Malaya, Kuala Lumpur 50603, Malaysia

Introduction

Coumarin is one of the aromatic compounds under the heterocyclic category that exhibits photoluminescence behavior. There are numerous coumarin derivatives mainly with various substituted groups at different positions that are potentially useful for many purposes. These include the control of cell cancer [1, 2], as a P-glycoprotein inhibitor [3], an iodine sensor [4], a fluorescence probe in thiol-disulfide exchange [5] and in the development of highly sensitive sensors [6]. The compound has also been incorporated in polymer matrices, demonstrating a fluorescence enhancement due to the stiffening of the dye structure and the intermolecular dipole-dipole interaction between the dopant and matrix [7]. In a more innovative way, coumarin has been used as a side-chain in polysiloxanes that photochemically alters the refractive index of the polymers [8]. This shows that coumarin would be a good candidate in a heterogeneous condition despite its simple fused aromatic structure.

The interesting function of coumarin has also been rolled out within self-assembled monolayers. There are examples of adsorbates with coumarin terminals directly assembling into a monolayer on polycrystalline gold substrate [9] and silicon wafer [10]. Chemical modification employing Cu(I)-catalyzed cycloaddition has produced similar monolayers [11]. Mixed monolayers partially containing coumarin on gold nanorods have been successfully produced from ligand exchange [12]. These have shown attempts to self-organize the coumarin into a more rigid structure. The overall flexibility of the assembled molecule may be reduced but such surfaces have been reported as an anisotropic phase, suggesting the importance of intermolecular and molecular packing [13–17].

The functionalization of self-assembled monolayers with coumarin derivatives is of interest due to their robust chromophore and tunable photodimerization at selected wavelengths

[9, 10]. The presence of coumarin chromophores on gold substrate was revealed by emission at 384 nm upon an excitation at 320 nm, suggesting that the fluorescence of coumarin is not quenched by electronic transition with the gold surface [9]. These findings are supported by the role of approximation of reactive groups within mixed self-assembled monolayers [18], and by fluorescence as an indicator of surface reactivity [19]. Besides, there must be chemical expressions other than photodimerization that display the potential of the structure as a part of a sensitive surface. For example, the fluorescence of metal-coumarin complexes has been investigated where the lactone of the coumarin is one of the chelation sites [6, 20]. It has been reported that the fluorescence of amino-coumarin derivatives is affected by the solute-solvent interaction [21]. In a different report, intermolecular and intramolecular hydrogen bonding has been suggested as a key factor in the fluorescence enhancement of aminobenzoic acid compounds [22]. However, evidence of the possible interaction occurring specifically between the lactone of the coumarin and its environment is still rather weak.

In this report, coumarin-terminated monolayer on silver was prepared from the chemisorption procedure in colloidal form. The arrangement of coumarin in a monolayer could form a relatively higher crystalline order of the moiety that would exert the lactone group away from the silver core. The lactone would thus be directly exposed to the solvent medium, while the rest of the molecule would be hindered from the environment (Scheme 1). Silver was chosen as a non-fluoresce particle with a high affinity surface for the formation of monolayers from alkyl disulphide compounds. Hypothetically, the emitted fluorescence from the coumarin termini could be tuned from the specifically accessible carbonyl group of the lactone with electrophilic or polar species.

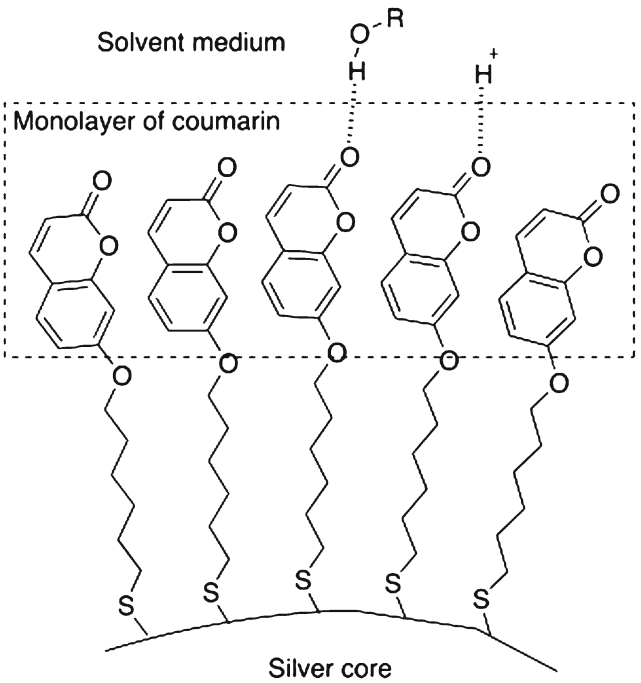

Scheme 1 Coumarin-terminated monolayer accommodates the carbonyl group closer to the solvent medium

Monolayer-protected silver particles were synthesized, as reported elsewhere, with minor modification [23]. The adsorbates were synthesized and purified as shown in Schemes 2 and 3 prior to the monolayer preparation procedure. The products were further analyzed to confirm the presence of an organic layer with coumarin moiety on silver particles. The fluorescence behavior of the colloidal sample was studied in different dispersion concentrations, solvents and pH.

Materials and Methods

Chemicals 11-bromoundecan-1-ol (97 %), potassium thioacetate (98 %), potassium hydroxide (99 %), sodium borohydride (96 %), tetradodecylammonium bromide (TDABr) (99.00 %) and silver nitrate (99.85 %) were purchased from Sigma Aldrich. Absolute ethanol, methanol, sodium sulphate anhydrous, magnesium sulphate anhydrous, sodium hydrogen carbonate, 7-hydroxycoumarin (98 %), 1,6-dibromohexane (97 %), hydrogen peroxide 30 %, acetone and toluene were purchased from Merck. Potassium carbonate (99.5 %) was purchased from R&M Chemicals. All chemicals were used as received.

Synthesis of 7-(6-bromohexyl-1-oxy)-2H-chromen-2-one (1) A mixture of 7-hydroxycoumarin (5.35 g, 33.0 mmol), 1,6-dibromohexane (8.05 g, 33.0 mmol) and potassium carbonate anhydrous (6.84 g, 49.5 mmol) in 150 ml dried acetone was refluxed overnight. The solvent was removed under vacuum. The crude product was washed with water and extracted with dichloromethane. The organic layer was dried over anhydrous magnesium sulphate and excess solvent was removed under vacuum. The crude was further purified over a silica gel column chromatograph with 1:1 chloroform-hexane eluent to afford 3.7 g (36 % yield) of a white solid. R_f=0.71 (1:1 hexane:ethyl acetate), m.p.: 53–55 °C. ^{1}H NMR (400 MHz, $CDCl_3$): δ 7.6 (d, J=9.5 Hz, Ar**H**, 1H) 7.3 (d, J=8.6 Hz, Ar**H**, 1H), 6.8 (dd, J= 6.4 Hz, Ar**H**, 1H), 6.7 (d, J= 2.2 Hz, Ar**H**, 1H), 6.2 (d, J=9.3 Hz, Ar**H** 1H), 3.9 (t, J= 6.3 Hz, **CH_2**O, 2H), 3.4 (t, J= 6.8 Hz, **CH_2**Br, 2H) 1.2–1.9 (m, **CH_2**, 8H). ^{13}C NMR (400 MHz, $CDCl_3$): 162.3, 161.2, 155.9, 143.4, 128.7, 114.9, 112.9, 112.6, 101.3, 68.4, 33.7, 32.6, 28.8, 27.9, 25.4. FTIR (cm^{-1}): 2943(s), 2864 (s), 1706 (s), 1613(s), 1468(s), 1131 (s). A.

Synthesis of 6-coumarinylhexylthiolate (2) A mixture of compound **1** (3.0 g, 9 mmol) and potassium thioacetate (1.26 g, 11 mmol) was stirred in 50 ml absolute ethanol for 24 h under nitrogen. The solvent was then removed under

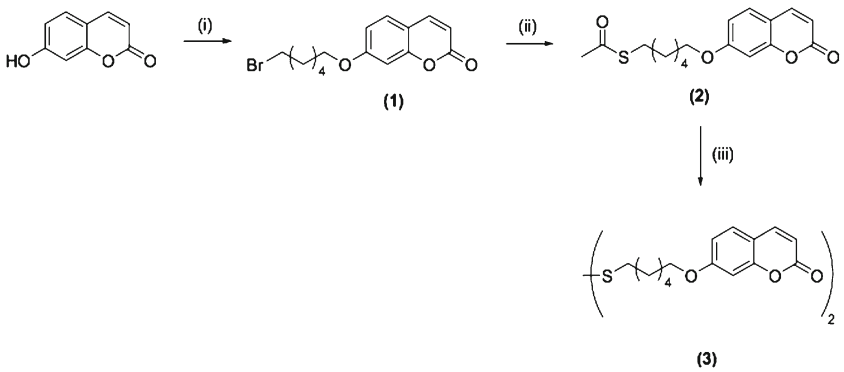

Scheme 2 Reaction pathway for the synthesis of bis(6-coumarinylhexyl) disulphide (**3**) from 7-hydroxylcoumarin. (*i*) 1,6-dibromohexane, K_2CO_3, dry acetone, r.t., overnight (*ii*) $KSOCH_3$, absolute ethanol, r.t., 12 h (*iii*) K_2CO_3, methanol-water mixture, r.t., 48 h

vacuum and the crude was dissolved in dichloromethane and washed with distilled water. The organic layer was dried over anhydrous magnesium sulphate. The excess solvent was removed under vacuum to produce 1.4 g (83 % yield) of white solid. R_f=0.87 (3:1 hexane:ethyl acetate), m.p.: 140–142 °C. ^{1}H NMR (400 MHz, $CDCl_3$): δ 7.5 (d, *J*=9.2 Hz, Ar**H**, 1H) 7.3 (d, *J*=8.8 Hz, Ar**H**, 1H), 6.8 (dd, *J*= 8.4 Hz, Ar**H**, 1H), 6.7 (d, *J*= 1.6 Hz, Ar**H**, 1H), 6.2 (d, *J*=9.6 Hz, Ar**H** 1H), 3.9 (t, *J*= 6.8 Hz, **CH$_2$**O, 2H), 2.8 (t, *J*=7.6 Hz, **CH$_2$**SCOCH$_3$, 2H), 2.3 (s, SCO**CH3**, 3H), 1.1–1.6 (m, **CH$_2$**, 8H). FTIR (cm^{-1}): 2937 (s), 2858 (s), 1708 (s), 1610(s), 1428 (s) 1124(s), 1016(s).

Synthesis of Bis(6-coumarinylhexyl) Disulfide (3) Compound **2** (0.5 g, 1.5 mmol) was dissolved in 10 ml solvent mixture (4:1 methanol-water) in the presence of 0.65 g (5 mmol) potassium carbonate, and stirred over 2 days, at room temperature. The solvent was then removed under vacuum and the residue was dissolved in 70 ml dichloromethane. The organic layer was washed with 100 ml of water a couple of times. The organic layer was dried over anhydrous magnesium sulphate. The excess solvent was removed under vacuum to obtain 0.2 g of white solid (48 % yield). R_f=0.4 (2:1 hexane:ethyl acetate), m.p.: 120–122 °C. ^{1}H NMR (400 MHz, $CDCl_3$): δ 7.6 (d, *J*=9.5 Hz, Ar**H**, 2H) 7.4 (d, *J*=8.6 Hz, Ar**H**, 2H), 6.8 (dd, *J*= 8.6 Hz, Ar**H**, 2H), 6.7 (d, *J*= 2.2 Hz, Ar**H**, 2H), 6.2 (d, *J*=9.5 Hz, Ar**H** 2H), 3.9 (t, *J*= 6.6 Hz, **CH$_2$**O, 4H), 2.6 (t, *J*=7.3 Hz, **CH$_2$**S, 4H), 1.2–1.8 (m, **CH$_2$**, 16H). ^{13}C NMR (400 MHz, $CDCl_3$): 162.3, 161.3, 155.9, 143.4, 128.7, 113.0, 112.5, 101.3, 68.4, 50.0, 38.9, 29.0, 28.9, 28.2, 25.7. FTIR (cm^{-1}): 2930 (s), 2856 (s), 1699 (s), 1603(s), 1433 (s) 1125 (s). LCMS: *m/z* 555 [M+H$^+$]. Anal. Calcd. for $C_{30}H_{34}O_6S_2$: C, 64.96; H, 6.18; O, 17.31; S, 11.56. Found: C, 64.19; H, 6.29; S, 11.50.

Synthesis of 11-thioacetylundecan-1-ol (4) A mixture of 1-bromoundecanol (5 g, 0.02 mol) and potassium thioacetate (2 g, 0.02 mol) was dissolved in 100 ml absolute ethanol and stirred at room temperature for 48 h. The crude was collected from solvent evaporation and dispersed in a buffer solution of sodium hydrogen carbonate (100 ml). The product was extracted from 100 ml diethyl ether 3 times. The organic layer was washed with distilled water (100 ml×2) and dried over sodium sulphate anhydrous. The excess solvent was removed under vacuum to obtain 4.89 g of 11-thioacetylundecan-1-ol (97.8 % yield). R_f=0.74 (1:1 hexane:ethyl acetate), m.p.: 105–107 °C. ^{1}H NMR (400 MHz, $CDCl_3$): δ 3.6 (t, *J*= 6 Hz, **CH$_2$**OH, 2H), 2.8 (t, *J*=7.6 Hz, **CH$_2$**SOCH$_3$, 2H), 2.3 (s, **CH$_3$**O, 3H), 1.4–1.2 (m, **CH$_2$**, 18H). FTIR (cm^{-1}): 3369 (br), 2920 (s), 2851 (s), 1688 (s), 1466 (s). Anal. Calcd. for $C_{13}H_{26}O_2S$: C, 63.37; H, 10.64; O, 12.99; S, 13.01. Found: C, 62.67; H, 10.71; S, 12.06.

Synthesis of Bis(11-hydroxyundecyl) Disulfide (5) 11-thioacetylundecan-1-ol **(9)** (4 g, 16 mmol) was mixed with a solution of potassium hydroxide (2 g, 37 mmol) in methanol (30 ml). Then, 30 % hydrogen peroxide solution (4 g, 117 mmol) was added to the mixture and stirred at 50 °C for 1 h. When the mixture had cooled down to room temperature, the compound was extracted with diethyl ether (3×10 ml) and washed with 5 % HCl aqueous solution (2×10 ml). The organic solution was dried up over anhydrous sodium sulphate. Evaporation of the solvent yielded 2.13 g white solid (53 % yield). R_f=0.37 (2:1 hexane:ethyl acetate), m.p: 64–66 °C. ^{1}H NMR (400 MHz, $CDCl_3$): δ 3.6 (t, *J*=6.6 Hz, **CH$_2$**OH, 4H), 2.6 (t, *J*=7.4 Hz, **CH$_2$**S, 4H), 1.2–1.6 (m, **CH$_2$**, 36H). ^{13}C NMR (400 MHz, $CDCl_3$): 63.1 (**CH$_2$**OH), 39.2 (**CH$_2$**S), 32.8–25.7 (**CH$_2$**). FTIR (cm^{-1}): 3367(br), 2918 (s), 2850 (s), 1470 (s). LCMS: *m/z* 407 [M+H$^+$]. Anal. Calcd. for

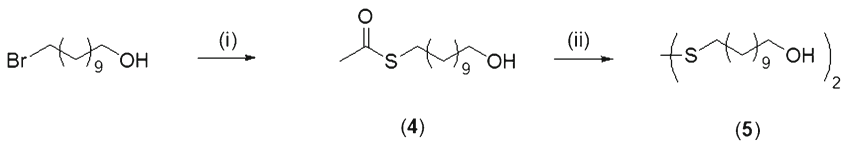

Scheme 3 Preparation of bis(11-hydroxyundecyl) disulfide (**5**) begin from 11-bromoundecan-1-ol as a pre-cursor. (*i*) $KSOCH_3$, ethanol, under nitrogen, r.t., 48 h and (*ii*) KOH, H_2O_2, 50 °C, 1 h

$C_{22}H_{46}O_2S_2$: C, 64.97; H, 11.40; O, 7.87; S, 15.77. Found: C, 64.87; H, 12.26; S, 15.38.

Preparation of Coumarinyl-Terminated Self-Assembled Monolayer (C-SAM) An appropriate amount of tetradodecylammonium bromide was dissolved in 6 ml toluene to produce approximately 0.1 M of surfactant solution. The solution was added into a vigorously-stirred silver nitrate aqueous solution (10 ml, 0.03 M). The upper layer turned into a cloudy light yellow solution. The mixture was then repeatedly shaken to reduce the size of the water droplets. The layers were left to settle and the organic phase collected. A solution of compound **3** (0.062 mmol, 0.0344 g) in 5 ml toluene was injected into the organic phase, followed by sodium borohydride aqueous solution (8 ml, 0.4 M). The reaction mixture was further stirred for 24 h in ambient condition. The organic phase was collected and concentrated to about 5 ml under vacuum. 250 ml methanol was added to the mixture and refrigerated overnight for effective precipitation of silver nanoparticles. The black suspension was separated after being centrifuged for 10 mins at 6000 rpm. The crude was washed with ethanol and centrifuged again to collect 0.02 g of particle.

Preparation of Hydroxyl-Terminated Self-Assembled Monolayer (H-SAM) A similar procedure to the above was applied to produce **H-SAM,** with compound **3** replaced by compound **5**. In this preparation, a solution of compound **5** (0.12 mmol, 0.0491 g) in 12 ml methanol was injected into the organic phase followed by the reduction procedure.

Instrumentations and Sample Preparations The IR absorption spectra of all samples were recorded on Perkin Elmer RX1 spectrophotometer with the assistance of ATR sampling technique. The UV-Visible absorptions were carried out using Cary 60 UV-vis spectrophotometer at room temperature in a standard 1-cm quartz cell. The sample absorptions were determined at a concentration of 0.25 mg/ml. The average size of the dispersed particles was determined using Malvern Zetasizer Nano Z. The samples used for particle size were prepared at 0.01 mg/ml in ethanol. The morphological and elemental studies of the samples were examined using a scanning electron microscope (model FEI Quanta 450FEG) equipped with energy-dispersive Spectrometer (model Oxford Aztec).

The fluorescence data of the samples with various dispersion concentrations were collected using a Cary Eclipse Fluorescence spectrophotometer at room temperature, with standard 4 windows 1-cm quartz cuvette. The excitation wavelengths of the samples were acquired from dispersions at 0.01 mg/ml in ethanol and chloroform under Cary 60 UV-Visible spectrophotometer. All samples for different dispersion concentrations were prepared in ethanol and chloroform in a 5-ml volumetric flask from the initially-prepared stock dispersion solution (0.25 mg/ml). A series of samples was prepared with different pH at 0.01 mg/ml from stock solution (0.02 mg/ml) in an equal volume of distilled water-ethanol. The pH of the samples was adjusted by adding hydrochloric acid (0.01 M) and sodium chloride (0.01 M) while directly probed under a pH meter. The width for excitation and emission slits used for all fluorescence measurement was 10 nm.

Results and Discussion

Formation of Coumarin-Terminated Monolayer on Silver Particles (C-SAM)

Products of the reduction of silver ions in the presence of disulphide compounds using phase transfer method [24] were analyzed under FTIR prior to the preparation of dispersion. A signal at 1708 cm^{-1} was assigned for C=O stretching, while the signal at around 1600 cm^{-1} indicated the presence of C=C stretching from the aromatic group. Such a signal was not observed in **H-SAM**. The signals at 2914 and 2846 cm^{-1} indicated the presence of C-H vibration in both **C-SAM** and **H-SAM**. It has been reported that the determination of crystalline-ordered saturated alkyl chain on flat self-assembled monolayer requires a higher transmittance frequency of about 2920 cm^{-1} due to the domination of *trans*--conformation [25]. Although the adsorbate compound **3** had bulky coumarin, the **C-SAM** product showed the consistency of an acceptable crystalline order of an organic monolayer. A significant decrement of signals at 616 and 604 cm^{-1} in both **C-SAM** and **H-SAM** respectively most probably indicated the absent of S-S stretching that initially observed in their respective adsorbates [26]. In order to further justify the formation of Ag-S, the samples were analyzed under ordinary Raman in between 200 and 300 cm^{-1}. The spikes at 297 and 215 cm^{-1} indicated the presence of Ag-S stretching in both **C-SAM** and **H-SAM** [27]. This was an early indication of the chemisorption of disulphide compounds on the silver particles.

C-SAM was further analyzed under SEM-EDS. The micrograph of **C-SAM** particles showed the clusters of particle with various diameters (Fig. 1). However, the size distribution of the particles was determined by particle sizer and not by this technique. The spherical shape of the **C-SAM** particles was noticeable, indicating less interaction between the particles in the target product. This was possibly due to the presence of heterocyclic terminal of the coumarin in **C-SAM**. Although there was no further evidence of the diameter range of both particles obtained from this technique, silver particles of a reasonable size for the formation of self-assembled monolayer had been successfully produced.

The atomic percentage of carbon, oxygen, sulfur and silver of **C-SAM** was identified from EDS. The average reading was

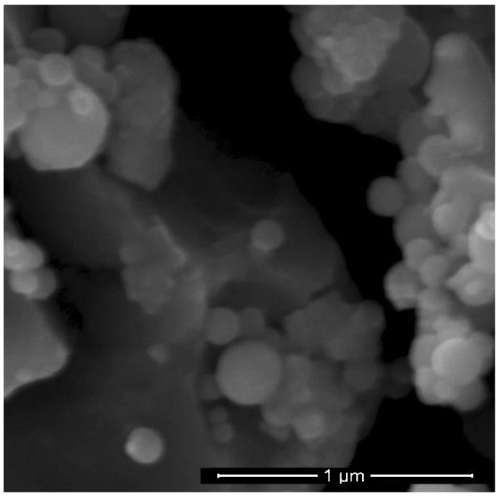

Fig. 1 SEM images of silver particles produced in the presence of compound **3**

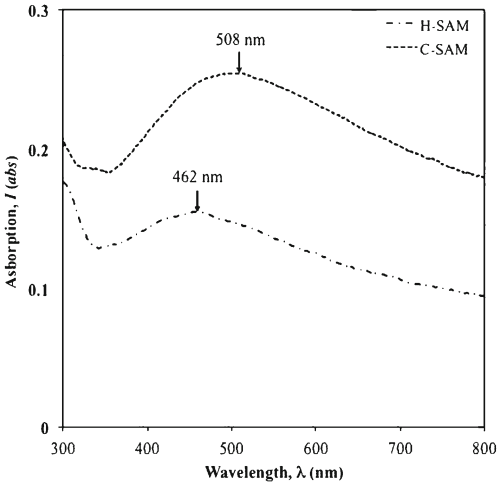

Fig. 2 UV-visible spectra showed absorption of silver nanoparticles with the monolayer of compound **3** (**C-SAM**) (*top*) and silver nanoparticles with the monolayer of compound **5** (**H-SAM**) (*bottom*)

obtained from at least five points of measurement. Sulfur with 4.16 %±0.44 was chosen as a reference element because each adsorbate molecule in the monolayer should contain a single sulfur atom anchored to a silver atom. 47.87 %±0.44 carbon atoms were determined with 11.5 carbon to sulfur ratio. Oxygen and silver were determined as 4 units (17.21 %±0.72) and 7.4 units (30.96 %±1.71) respectively. The results were also consistent with the measurement from the weight percentage. The ratio of carbon to sulfur was 12.4 (14.13 %±1.18), oxygen to sulfur 4.4 (6.74 %±0.42) and silver to sulfur 7.4 (76.09 %±0.71). The weight percentage of the sulfur was detected as 3.03 %±0.09. All ratios of the organic part were determined from atomic and weight percentages and very close to the calculated ratio ($C_{15}O_3S$). The results also revealed that the particle consisted of 7-fold higher atomic silver than did the adsorbate molecule. These results suggested that the adsorbates were successfully chemisorbed onto the silver particles with a reasonable size of the particles in order to form a protective organic layer with coumarin terminal.

The following analyses were carried out for the particles in dispersion form under a particle sizer and UV-visible spectrophotometer. The average sizes of **C-SAM** and **H-SAM** were determined at 138.4 nm and 131.7 nm respectively. Both suspensions showed a moderate polydispersity index of 0.393 for **C-SAM**. These results showed good agreement with the micrograph SEM image and the broadened absorption UV-visible spectra of the dispersion. The absorption observed for **C-SAM** was 508 nm, higher than the 462 nm wavelength recorded for **H-SAM** (Fig. 2). There were reports on a qualitative relation between the size of particles and the width of absorbance peak, where narrower absorption peak denoted smaller diameter silver particles [28, 29]. It had also been reported earlier that the dispersion of monolayer on silver particles exhibited an absorption band in the range of 400 and 500 nm, while unprotected silver nanoparticles were known to exhibit a maximum absorption band of about 390 nm [30]. The shift in the maximum wavelengths was due to the surface plasmon band of the particles resulting from the bond formation of the Ag clusters and the ligands. It was found that the shifting of the maximum wavelength was comparable for **C-SAM** and **H-SAM,** apparently because of the presence of heterocyclic coumarin within the monolayer on the silver surface. No further analysis was carried out to observe the particular shifting associated with the coumarin terminal.

These results showed good agreement with the broad absorption UV-visible spectra. The growth of the silver particles was successfully controlled and stabilized by the improvised size of the particles. Tetraoctylammonium bromide involved

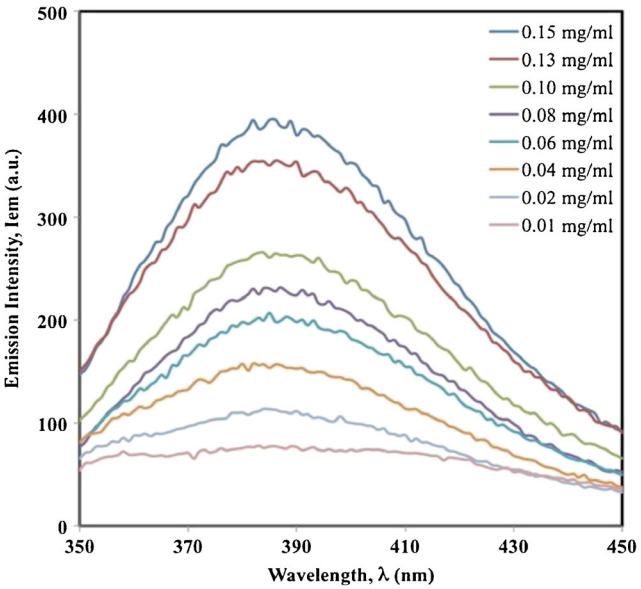

Fig. 3 The fluorescence emission spectra of **C-SAM** at different suspension concentrations

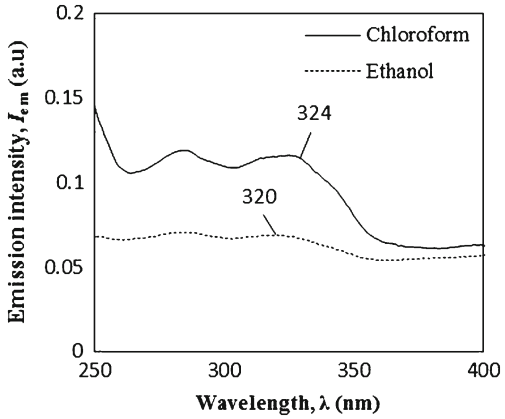

Fig. 4 Absorption spectra of **C-SAM** in different solvents

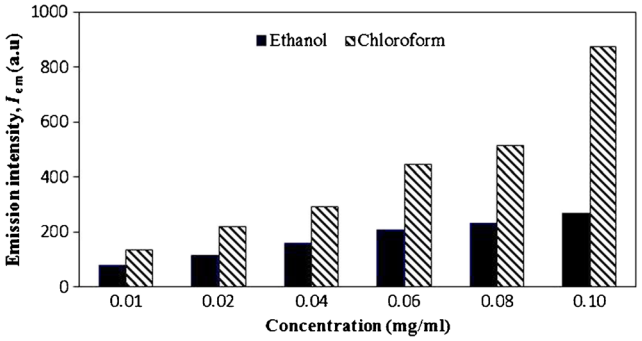

Fig. 6 Fluorescence of **C-SAM** was unaffected by the dispersion concentrations especially in chloroform

in the preparation of monolayer protected silver nanoparticles would control the growth rate, shape and size of particles [31]. The role of tetradodecylammonium bromide in the phase transfer process was pronounced but the mechanistic aspect to produce smaller water droplets and preventing them from fusing with each other could be improved, especially with regard to the preparation and condition. It clearly indicated that the addition of disulfide compounds during the preparation would further sustain the size of silver particles by forming an excellent protective organic layer.

Fluorescence Emission of C-SAM

The fluorescence behavior of **C-SAM** was investigated in dispersion form. The fluorescence emission of **C-SAM** was observed at 386 nm when excited at 320 nm (Fig. 3). The Stokes shift for **C-SAM** was calculated as 66 nm. It had been previously reported that the maximum emission wavelength of coumarin red shifted by 10 nm, due to the dimerization process after irradiation at 300 nm [9], thus eliminating any possibility of photodimerization of the coumarin. This suggested that the unaffected emission wavelength with lower intensity was caused by the arrangement of coumarin terminal as a result of monolayer formation. The maximum emission wavelength also retained upon the dilution, implying that the emission was directly related to the amount of particles without affecting the conformation and interaction between the coumarin moieties.

Since there was also no irradiation to promote dimerization in this experiment, lower fluorescence intensity emitted from **C-SAM** was probably the translation of coumarin congregation in the monolayer. There have been reports that *H*-type dyes arrangement would quench the fluorescence emission such as for porphyrin derivatives [32] and perylenetetracarboxylic amphiphiles [33]. The coumarin groups of **C-SAM** would behave in a similar way by $\pi-\pi$ stacking interaction. Despite the formation of moderately-packed self-assembled monolayer, a closer distance amongst the coumarin groups could allow them to reach one another and favor an *H*-type arrangement.

Solvents Effect on the Absorption of C-SAM

The absorption spectra of **C-SAM** in two different solvents were recorded and displayed as shown in Fig. 4. Only ethanol

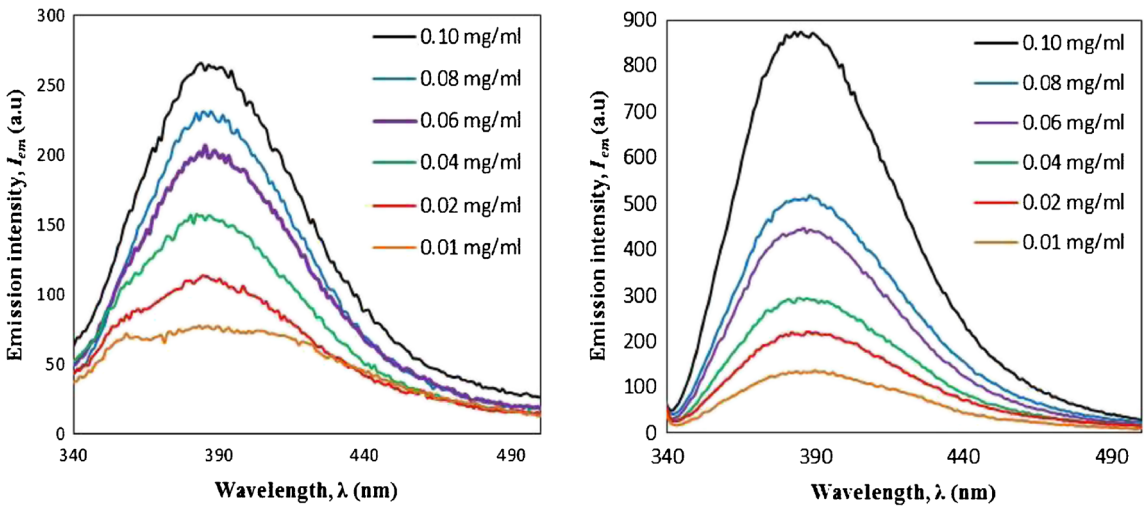

Fig. 5 Series of fluorescence of **C-SAM** were measured at different concentrations in ethanol (*left*) and in chloroform (*right*)

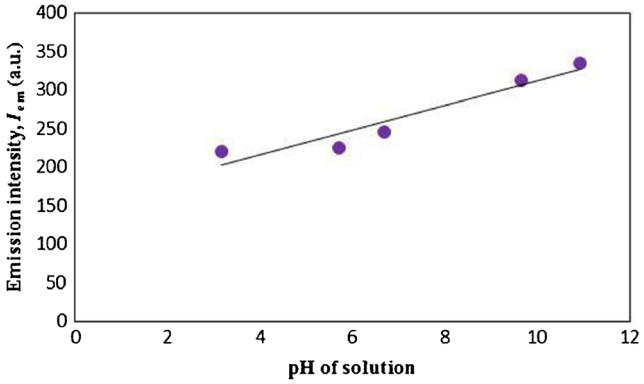

Fig. 7 Emission intensity of **C-SAM** increased from acidic to basic condition

and chloroform were used for the analysis due to the poor solubility of **C-SAM** in other less polar solvents. Absorption of the dispersion in chloroform was found to be much higher than it was in ethanol. Although both solvents could be good dispersion media for the particles, ethanol molecules could have better interaction with the carbonyl group. Two signals were observed from the spectra of **C-SAM** at about 284 and 320 nm, reflecting the aromatic and lactone groups respectively. The latter was chosen as an excitation wavelength in the fluorescence investigation because it promoted higher emission intensity.

Fluorescence of the samples was excited at 320 and 324 nm in ethanol and chloroform respectively. It was found that both the maximum fluorescence wavelengths in the two solvents were shown as a single band in the range of 380–390 nm (Fig. 5). The observed fluorescence emission trend of **C-SAM** in ethanol was similar to the fluorescence of **C-SAM** in ethanol but the fluorescence intensity of the sample at 0.01 mg/ml in chloroform was 3-fold higher than in ethanol in similar concentrations.

The intensity of the maximum emission from **C-SAM** in different solvents was plotted upon the dispersion concentration (Fig. 6). It has been well accepted that emission of solute from organic fluorescent usually quenched at a higher concentration. In this case, the intensity of samples in both solvents was almost directly proportionate to the concentration of the dispersion, even at higher concentrations. These probably indicated that the emission of coumarin in monolayer was not affected by the aggregation and collision behaviour of the particles.

The emissions intensities of **C-SAM** in the two solvents however, did not match. All emission intensities of the samples in ethanol were lower than those in chloroform. This was probably due to the quenching effect of a polar and a protic solvent, causing the formation of hydrogen bonding between the coumarin in monolayer and in ethanol. A protic polar solvent could form a strong hydrogen bond with lone electron pairs in solute [34]. This phenomenon favored the low-lying $n \rightarrow \pi^*$ transitions, which referred to the excitation of a non-bonding electron as an anti-bonding orbital. Thus, it propelled the excited state of the fluorophore into a higher energy level.

pH Effect on the Fluorescence of C-SAM

The results from UV-visible absorption and fluorescence emission of the **C-SAM** in organic solvents have directed our verdict on the role of interaction between the carbonyl group and the environment especially in hydrogen bonding. These triggered our curiosity to investigate dispersion in acid and base conditions. The fluorescence emissions of **C-SAM** in different pH were recorded and the emission intensity against pH was plotted as shown in Fig. 7. The intensity of the emission of **C-SAM** dispersion at pH neutral showed at about 250 a.u., close to the intensity from C-SAM in ethanol. This suggested that the mixed aqueous-alcohol medium at neutral would have a similar effect on ethanol environment.

The emission intensity of the **C-SAM** was lower in acidic than in basic, indicating a strong correlation to the amount of proton (H^+) in the solution. The proton species more easily interacted with the carbonyl group to form hydrogen bonding provided the lactone was elevated on the monolayer surface towards the aqueous medium. Therefore, the protonation of

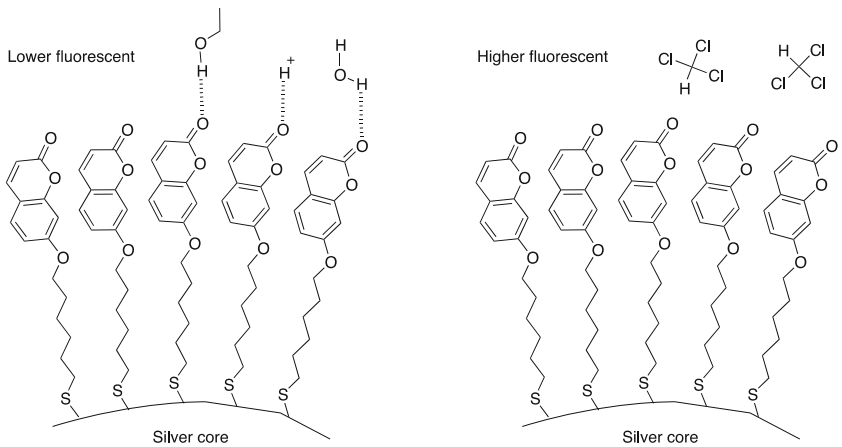

Fig. 8 Coumarin-terminated monolayer on silver particles may represent a well-arranged and localized heterocyclic group that restricted the carbonyl to interact with the solvent environment

non-bonded electrons from the carbonyl could be considered for the fluorescence quenching in acidic condition. A similar reason could be given for the **C-SAM** in basic condition where the interaction between the carbonyl and the positive species reduced gradually from the surface of the monolayer.

The results have indicated that a heterocyclic terminated monolayer with lactone moiety like coumarin could be self-assembled and well-organized on metallic particles (Fig. 8). The localized arrangement divided the monolayer into a simple region: the internal monolayer and the outer layer. The latter would be the region that primarily bore with the environment. The finding has shown the potential of carbonyl to interact strongly with the solvent environment. These situations should be taken into consideration when developing a sensitive device or sensor-based self-assembled monolayer especially involving analytes in a protic solvent or an aqueous media.

Conclusion

The formation of monolayers with heterocyclic and aromatic terminal on a metal surface has been demonstrated by using coumarin on silver particles. The arrangement of coumarin as a fluorescent terminal within the monolayer exerted the carbonyl group to the outer region that exposed them to the solvent environment. Hydrogen bonds between the exposed carbonyl and a protic solvent or proton in an aqueous would reduce fluorescence emission while the maximum emission wavelength was preserved. The elimination of the interaction from the surface of a monolayer, such as the dispersion in chloroform, would be an alternative to improve fluorescence properties in the selection of suitable polymers for composite formulation, in designing a fluorescence-based sensor and for developing fluorescent-doped pigments.

Acknowledgments The team acknowledges with thanks the financial support from the Postgraduate Student Grant Scheme (PG090-2012B) and the Fundamental Research Grant Scheme (MO002/2014).

We also thank Prof Rauzah Hashim for allowing us the use of important instruments under the HIR grant (UM.C/625/HIR/MOHE/05).

References

1. Thati B, Noble A, Creaven BS, Walsh M, McCann M, Devereux M, Egan DA (2009) Role of cell cycle events and apoptosis in mediating the anti-cancer activity of a silver (I) complex of 4-hydroxy-3-nitrocoumarin-bis(phenanthroline) in human malignant cancer cells. Eur J Pharmacol 602:203–214
2. Chen Y, Liu HR, Liu HS, Cheng M, Xia P, Qian K, Lee KH (2012) Antitumor agents 292. Design, synthesis and pharmacological study of S-and O-substituted 7-mercapto-or hydroxy-coumarins and chromones as potent cytotoxic agents. Eur J Med Chem 49: 74–85
3. Lee K, Chae SW, Xia Y, Kim NH, Kim HJ, Rhie S, Lee HJ (2014) Effect of coumarin derivative- mediated inhibition of P-glycoprotein on oral bioavailability and therapeutic efficacy of paclitaxel. Eur J Pharmacol 723:381–388
4. Mahapatra AK, Hazra G, Roy J, Sahoo P (2011) A simple coumarin-based colorimetric and ratiometric chemosensor for acetate and a selective fluorescence turn-on probe for iodide. J Lumin 131:1255–1259
5. Cao X, Lin W, Yu Q (2011) A ratiometric fluorescent probe for thiols based on a Tetrakis (4- hydroxyphenyl) porphyrin–Coumarin scaffold. J Org Chem 76:7423–7430
6. Ahmed S, Al-Kady GM, Mohamed MH, El-Zeiny ME (2009) Fluorescence enhancement of coumarin thiourea derivatives by Hg^{2+}, Ag^{+}, and silver nanoparticles. J Phys Chem 113:9474–9484
7. Donovalova J, Cigan M, Stankovicova H, Gaspar J, Danko M, Gaplovsky A, Hrdlovic P (2012) Spectral properties of substituted coumarins in solution and polymer matrices. Molecules 17:3259–3276
8. Schraub M, Soll S, Hampp N (2013) High refractive index coumarin-based photorefractive polysiloxanes. Eur Polym J 49: 1714–1721
9. Li W, Lynch V, Thompson H, Fox MA (1997) Self-assembled monolayers of 7-(10-thiodecoxy) coumarin on gold: synthesis, characterization, and photodimerization. J Am Chem Soc 119: 7211–7217
10. Fang J, Whitaker C, Weslowski B, Chen MS, Naciri J, Shashidhar R (2001) Synthesis and photodimerization in self-assembled monolayers of 7-(8-trimethoxysilyloctyloxy) coumarin. J Mater Chem 11:2992–2995
11. Haensch C, Hoeppener S, Schubert US (2008) Chemical surface reactions by click chemistry: coumarin dye modification of 11-bromoundecyltrichlorosilane monolayers. Nanotechnology 19: 035703
12. Mlambo M, Mdluli PS, Shumbula P, Mpelane S, Moloto N, Skepu A, Tshikhudo R (2013) Synthesis and characterization of mixed monolayer protected gold nanorods and their Raman activities. Mater Res Bull 48:4181–4185
13. Cunha F, Tao NJ, Wang XW, Jin Q, Duong B, D'Agnese J (1996) Potential-induced phase transitions in 2, 2′-bipyridine and 4, 4′-bipyridine monolayers on Au (111) studied by in situ scanning tunneling microscopy and atomic force microscopy. Langmuir 12: 6410–6418
14. Cunha F, Jin Q, Tao NJ, Li CZ (1997) Structural phase transition in self-assembled 1, 10′ phenanthroline monolayer on Au (111). Surf Sci 389:19–28
15. Tao NJ, DeRose JA, Lindsay SM (1993) Self-assembly of molecular superstructures studied by in situ scanning tunneling microscopy: DNA bases on gold (111). J Phys Chem 97:910–919
16. Jin Q, Rodriguez JA, Li CZ, Darici Y, Tao NJ (1999) Self-assembly of aromatic thiols on Au (111). Surf Sci 425:101–111
17. Ulgut B, Zhao Y, Grose JE, Ralph DC, Abruña HD (2006) Electrochemical properties of self-assembled monolayers of polyaniline: effects of the thiol substituent and reduced dimensionality. Langmuir 22:4433–4437
18. Chechik V, Crooks RM, Stirling CJM (2000) Reactions and reactivity in self-assembled monolayers. Adv Mater 12:1161–1171
19. Fox MA, Li W, Wooten M, McKerrow A, Whitesell JK (1998) Fluorescence probes for chemical reactivity at the interface of a self-assembled monolayer. Thin Solid Films 327:477–480
20. Tang J, Zhou L, Ma F, Yang C, Zhou JH (2012) Synthesis and luminescence properties of nanoparticles embedded with Europium (III) /coumarin complexes. J Optoelectron Adv Mater 14:84–89
21. Zakerhamidi MS, Ghanadzadeh A, Tajalli H, Moghadam M, Jassas M (2010) Substituent and solvent effects on the photo-physical

properties of some coumarin dyes. Spectrochim Acta A Mol Biomol Spectrosc 77:337–341
22. Zhou T, Li F, Fan Y, Song W, Mu X, Zhang H, Wang Y (2009) Hydrogen-bonded dimer stacking induced emission of aminobenzoic acid compounds. Chem Commun 22:3199–3201
23. Kwi LJ, Young-Il L, In-Keun S, Jaewoo J, Yong OS (2006) Direct synthesis and bonding origin of monolayer-protected silver nanocrystal from silver nitrate through in situ ligand. J Colloid Interface Sci 304:92–97
24. Goulet PJ, Lennox RB (2010) New insights into Brust–Schiffrin metal nanoparticle synthesis. J Am Chem Soc 132:9582–9584
25. Bertilsson L, Liedberg B (1993) Infrared study of thiol monolayer assemblies on gold: preparation, characterization, and functionalization of mixed monolayers. Langmuir 9:141–149
26. Murty KVGK, Venkataramanan M, Pradeep T (1998) Self-assembled monolayers of 1, 4- benzenedimethanethiol on polycrystalline silver and gold films: an investigation of structure, stability, dynamics, and reactivity. Langmuir 14:5446–5456
27. Bensebaa F, Zhou Y, Brolo AG, Irish DE, Deslandes Y, Kruus E, Ellis TH (1999) Raman characterization of metal-alkanethiolates. Spectrochim Acta A Mol Biomol Spectrosc 55:1229–1236
28. Shon YS, Cutler E (2004) Aqueous synthesis of alkanethiolate-protected Ag nanoparticles using bunte salts. Langmuir 20:6626–6630
29. He S, Yao J, Jiang P, Shi D, Zhang H, Xie S, Gao H (2001) Formation of silver nanoparticles and self- assembled two-dimensional ordered superlattice. Langmuir 17:1571–1575
30. Shon YS (2004) Metal nanoparticles protected with monolayers: synthetic methods. In: Schwarz JA (ed) Dekker encyclopedia of nanoscience and nanotechnology, 1st edn. Marcel Dekker, pp.1–11
31. Jiang X, Yu A (2010) One-step approach for the synthesis and self-assembly of silver nanoparticles. J Nanosci Nanotechnol 10:7643–7647
32. Yang JH, Chen YM, Ren YL, Bai YB, Wu Y, Jang YS, Li TJ (2000) Identification of H-aggregate in a monolayer amphiphilic porphyrin–TiO 2 nanoparticle heterostructure assembly and its influence on the photoinduced charge transfer. J Photochem Photobiol A Chem 134:1–7
33. Wu H, Xue L, Shi Y, Chen Y, Li X (2011) Organogels based on J- and H-type aggregates of amphiphilic perylenetetracarboxylic diimides. Langmuir 27:3074–3082
34. Schulman S (1977) Fluorescence and phosphorescence spectroscopy: physicochemical principles and practice. Pergamon Press, New York